Biointerface Research in Applied Chemistry
Open-Access Journal (ISSN: 2069-5837)

Article
Volume 13, Issue 4, 2023, 393
https://doi.org/10.33263/BRIAC134.393

Antibacterial Properties of Graphene and its Reinforcement Effect on Compressive Properties of PMMA

Abdul Manaf Abdullah [1,*], Dasmawati Mohamad [2,*]

[1] School of Mechanical Engineering, College of Engineering, Universiti Teknologi MARA, 40450 Shah Alam, Selangor, Malaysia. abdulmanaf@uitm.edu.my (A.M.M.);
[2] School of Dental Sciences, Health Campus, Universiti Sains Malaysia, 16150 Kubang Kerian, Kelantan, Malaysia, dasmawati@usm.my (D.M.);
* Correspondence: abdulmanaf@uitm.edu.my (A.M.A); dasmawati@usm.my (D.M);

Scopus Author ID 56890467100
Received: 18.06.2022; Accepted: 17.07.2022; Published: 1.11.2022

Abstract: Graphene and its derivatives have received significant attention due to their outstanding properties. This study aims to evaluate the antibacterial properties of graphene and its reinforcement effect on the mechanical properties of polymethyl methacrylate (PMMA) for potential bone substitution. The morphology of graphene was initially observed via a field emission scanning electron microscope (FESEM). Five concentrations of graphene (1, 0.5, 0.25, 0.125, and 0.0625 mg/mL) were then prepared, and its antibacterial properties were assessed against *Staphylococcus aureus*. Two concentrations that exhibited the highest antibacterial properties were selected and incorporated with PMMA. Graphene exhibited superior antibacterial properties at 0.5 and 1.0 mg/mL concentrations. The 0.5 mg/mL graphene-reinforced PMMA presented an increment of compressive strength by up to 48% and a compressive modulus of 72% compared to unfilled PMMA. In conclusion, the PMMA composite with improved biological and mechanical performance could be potentially used as a bone substitution.

Keywords: graphene; PMMA composite; antibacterial properties; compressive properties.

1. Introduction

The discovery of nanoparticles (NPs) has steered the direction of various research for years to come [1,2]. NPs are classified into numerous categories such as size, shape [3], application as well as properties [4], where chemical and physical properties are the most common classification [5]. Besides metal and ceramics, carbon-based NPs are getting significant attention owing to their outstanding electrical [6], physicomechanical, thermal [7], chemical, and biological [8] properties. Carbon-based NPs range from carbon nanotube (CNT), graphite, diamond, fullerene, carbon dot, and graphene, where graphene is the thinnest two-dimensional (2D) monolayer sp2 hybridized carbon atoms.

Graphene has been evaluated for various applications such as optoelectronics [9], biosensors [10] as well as biomaterials [11] due to its versatility. The demand for a biomaterial with considerable mechanical and antibacterial properties requires modification to the currently available biomaterials to exploit the potential of graphene to cater to the needs. It should be noted that graphene derivatives, particularly graphene oxide (GO) and reduced graphene oxide (rGO) [12], are well known for their excellent antibacterial efficacy against various bacteria due to the presence of functional groups. However, the antibacterial activity of non-

functionalized graphene is less reported, and the available findings on their mechanical properties are also varied [13,14].

This study was carried out to evaluate the antibacterial properties of graphene against Gram-positive bacteria of *Staphylococcus aureus* (*S. aureus*). *S. aureus* is one of the most prominent pathogens that cause human infection. Besides, the effect of graphene incorporation on the mechanical properties of polymeric biomaterial was also elucidated. In this study, a widely used biomaterial of polymethyl methacrylate (PMMA) was selected to improve its mechanical performance to be suited for bone substitution.

2. Materials and Methods

2.1. Materials.

In this study, brain heart infusion (BHI) broth (CM 1135, OXOID, UK) and *Staphylococcus aureus* (*S. aureus*) (ATCC 25923, ATCC, USA) were used for the evaluation of antibacterial properties of Graphene nanoplatelets (0544DX, SkySpring Nanomaterials Inc, USA). Meanwhile, polymethyl methacrylate (PMMA) powder and methyl methacrylate (MMA) monomer (Palacos® R, Heraeus Medical GmbH, Germany) were used for the preparation of graphene-filled PMMA.

2.2. Morphological analysis.

The microstructure of graphene was observed using a field emission scanning electron microscope (FESEM) (Quanta 450, FEG, Netherlands). Prior to the morphological observation, the graphene nanoplatelets were dispersed on a stub and gold-sputtered using a sputtering machine (EM SDD005, Leica, Germany).

2.3. Antibacterial study.

A bacterial suspension of 0.5 McFarland was initially prepared prior to dilution with BHI broth at a ratio of 1:150 to produce a bacterial colony of 1×10^6 CFU/mL. Graphene nanoplatelets were ultraviolet (UV) irradiated for 30 minutes, followed by the preparation of five concentrations (2, 1, 0.5, 0.25, and 0.125 mg/mL) of graphene suspension. 100 µL of graphene suspension was inoculated with 100 µL of bacterial suspension in a 96-well plate, resulting in final concentrations of 1, 0.5, 0.25, 0.125, and 0.0625 mg/mL. The bacterial growth represented by the optical density was measured hourly (until 7 hours) using a microplate reader at 570 nm.

2.4. Moulds preparation.

A rectangular mold of 36 × 18 × 12 mm embedded with 3 cylinders of 12 and 6 mm in height and diameter was initially designed using computer-aided design software (Solidworks 2013, Solidworks, USA). The designed file was printed using multi-jet modeling (MJM) 3D printer (Objet 30 Scholar, Stratasys, USA). The designed mold and its 3D printed part are shown in Figure 1.

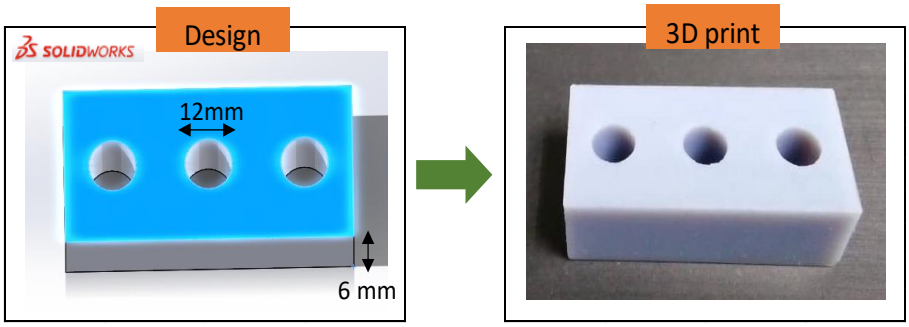

Figure 1. The designed mold and its 3D printed part.

2.5. Specimen preparation.

The compressive specimens (n=3/group) were prepared by mixing liquid and powder components of MMA and PMMA at a ratio of 1:2, following the manufacturer's instructions. Two concentrations of graphene that exhibited the highest antibacterial properties were selected and incorporated into the MMA liquid. The liquid of MMA, graphene, and the powder component of PMMA were mixed for 30 seconds in a silicone rubber bowl. The homogenous, non-sticky dough was then introduced into a 3D-printed mold and left for 10 minutes. Unfilled PMMA was also prepared as a control. The hardened unfilled, and graphene-filled PMMA were removed from the mold upon completion.

2.6. Determination of compressive properties.

The compressive strength and modulus of unfilled and graphene-filled PMMA were determined utilizing a universal testing machine (Shimadzu AGX-2plus, Shimadzu, Japan) fitted with a 20 kN load cell at a cross-head speed of 1 mm/min.

3. Results and Discussion

3.1. Graphene morphology.

An understanding of the morphological properties of graphene is deemed important to predict its behavior. The morphologies of graphene were observed via a FESEM. Figure 2(a) revealed the structure of the graphene, which was in a thin layer formed of butterfly wing alike particles. The diameters of the particles were approximately 10 µm. Graphene tended to lie horizontally, resulting in a high surface area. Graphene was also prone to stick to each other, Figure 2(b), which could be due to the presence of Van der Waals attraction between the 2D monolayers.

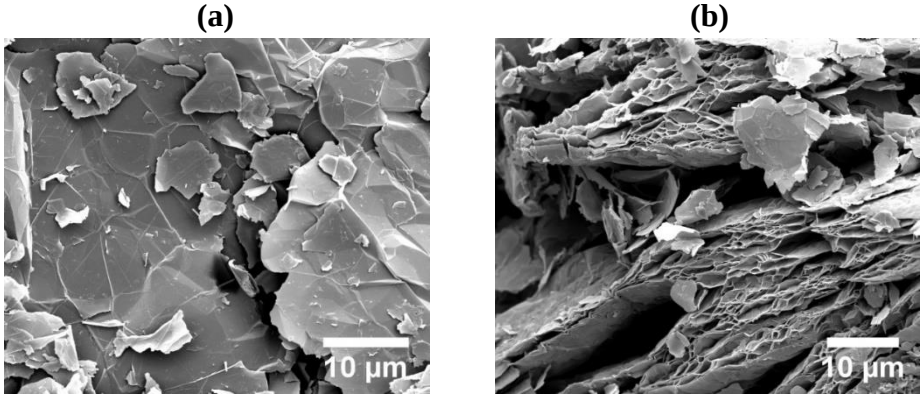

Figure 2. FESEM micrographs of graphene nanoparticles.

3.2. Antibacterial properties.

The antibacterial properties of graphene at different concentrations were assessed on Gram-positive bacteria of S. aureus. The growth curve of untreated and graphene-treated *S. aureus* is shown in Figure 3. In general, *S. aureus* started to grow rapidly after 3 hours and became plateaued after 6 hours of incubation.

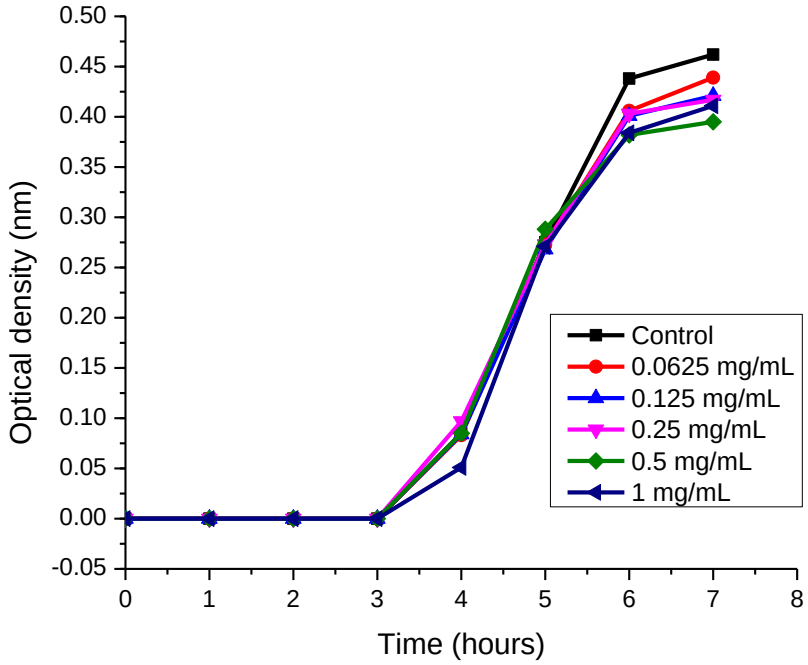

Figure 3. Growth curves of treated and untreated *S. aurues.*

After 3 hours of incubation, the growth curve of 1 mg/mL graphene's treated *S. aureus* seemed to deviate from others. A high graphene concentration is associated with bacterial capturing capability, where a high concentration tends to reduce the bacterial colony [15, 16]. However, the concentrations were not sufficient to depress the bacteria. Exponential growth was observed in all concentrations after 4 hours of incubation. The optical density of graphene-treated *S. aureus* (at 7 hours) generally decreased with the increase in graphene concentrations. However, the growth curve of 1 mg/mL graphene-treated *S. aureus* was slightly higher than 0.5 mg/mL graphene-treated *S. aureus*, so a further study could be performed to understand the phenomenon. Graphene presented a dose-dependent effect where concentrations of 0.5 and 1 mg/mL showed the most effective antibacterial properties. It should be noted that a similar detrimental effect is potentially harmful to the normal cells as well and that the cytotoxicity effect of these amounts against normal cells needs to be assessed in vitro to warrant the safety of the graphene. After being treated for 7 hours, graphene reduced the amount of S. aureus by 5 to 15%, indicating that graphene potentially impaired the growth of the bacteria. Graphene is able to penetrate the cell membrane and extract phospholipid-physical damage [17,18], which stemmed from the van der Waals interaction.

3.3. Compressive properties.

Compressive testing was performed to elucidate the reinforcement effect of graphene on the PMMA matrix. The mean compressive strength and modulus of unfilled and graphene-filled PMMA are summarised in Table 1.

Table 1. Compressive properties of PMMA composites

Graphene content (mg/mL)	Compressive strength (MPa)	Compressive modulus (MPa)
0	221.49 (89.74)	725.45 (444.83)
0.5	327.51 (21.35)	1248.93 (312.00)
1.0	192.22 (99.69)	1463.83 (78.62)

From the table, the incorporation of 0.5 mg/mL graphene increased the compressive strength by 48% compared to unfilled PMMA. However, additional graphene of up to 1.0 mg/mL caused the compressive strength to reduce by approximately 13% compared to unfilled PMMA. The highest compressive strength was recorded at 327.51 MPa (0.5 mg/mL graphene loading). It should be noted that the compressive strength of polymer composites typically depends on several factors, such as the dispersion of fillers and interfacial adhesion between fillers and polymer matrix. However, in this study, the natural structure of graphene, which can cover a high surface area, as shown in Figure 2, contributed to the reinforcement effect in the PMMA matrix. At the same time, the reduction of compressive strength at 1.0 mg/mL graphene loading could be due to the agglomeration of graphene. It should be noted that the incorporation of graphene, to a certain extent, reduces the strength of polymer composites [19, 20] as particles with a large surface area are likely to become clusters [21,22].

On the other hand, incorporating 0.5 and 1.0mg/mL graphene increased the compressive modulus by 72 and 102%, respectively. The highest compressive modulus was recorded at 1.0 mg/mL graphene loading (1463.38 MPa). It is a fact that fillers function to immobilize the polymer chain when exposed to external load graphene-filled PMMA presented a higher compressive modulus than unfilled PMMA. This phenomenon could be observed in Figure 4, where the slope of graphene-filled PMMA was steeper than the unfilled PMMA. The presence of graphene improved the efficiency of the PMMA to resist the deformation, resulting in an increase in the strain at break.

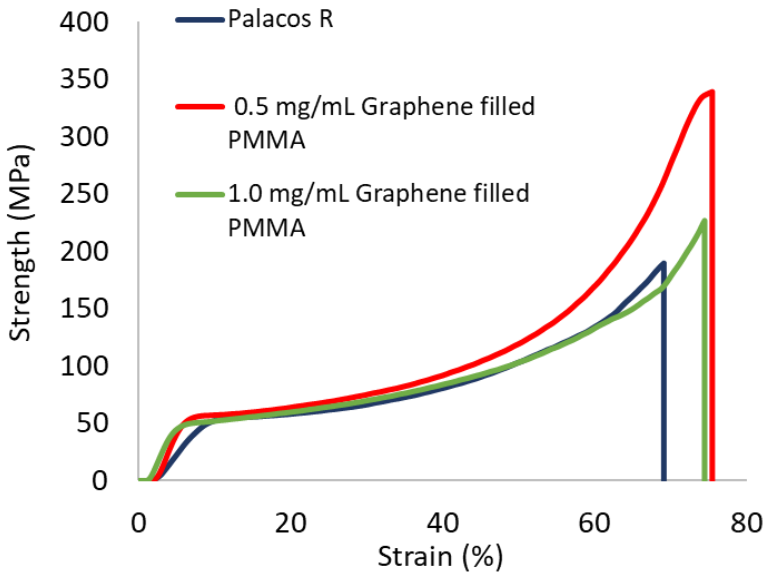

Figure 4. Stress-strain curves of PMMA and its composites.

While this study aims to introduce graphene-reinforced PMMA as bone substitution, care should be taken to compare its current mechanical performance with the mechanical properties of bone. It should be noted that the cortical bone has compressive strength and modulus of 130-200 MPa and 11.5-17 GPa, respectively [23-25]. Meanwhile, a trabecular bone exhibits an approximately 90% lower strength and modulus than the cortical bone. The PMMA composite at a graphene concentration of 0.5 mg/mL exhibited a compressive strength of 327.51 MPa, which exceeded the strength requirement of trabecular bone. However, the modulus of the composite needs to be improved further.

4. Conclusions

The antibacterial properties of graphene and its effect on the mechanical properties of PMMA were assessed. Graphene exhibited superior antibacterial properties at high concentrations. The graphene-reinforced PMMA exhibited higher mechanical properties than unfilled PMMA at a certain concentration, which could be attributed to the graphene's high surface area. The formulation could be further assessed to conform to the development regulations concerning biomaterials. With current mechanical and biological performance, the graphene-reinforced PMMA could be a potential candidate for bone substitution.

Funding

This research received no external funding.

Acknowledgments

The authors would like to acknowledge Mrs. Roziyani Hashim (Craniofacial Laboratory of School of Dental Sciences, Universiti Sains Malaysia) for the technical support during the biological experiment.

Conflicts of Interest

The authors declare no conflict of interest

References

1. Akasov, R.; Khaydukov, E.V.; Yamada, M.; Zvyagin, A.V.; Leelahavanichkul, A.; Leanse, L.G.; Prow, T.W.Dai, T. Nanoparticle Enhanced Blue Light Therapy. *Advanced Drug Delivery Reviews*, **2022**, 114198, https://doi.org/10.1016/j.addr.2022.114198.
2. Selmani, A.; Kovačević, D.Bohinc, K. Nanoparticles: From synthesis to applications and beyond. *Advances in Colloid and Interface Science*, **2022**, 102640, https://doi.org/10.1016/j.cis.2022.102640.
3. Rizwan, M.; Shoukat, A.; Ayub, A.; Razzaq, B.Tahir, M.B., *Chapter 3 - Types and classification of nanomaterials*, in *Nanomaterials: Synthesis, Characterization, Hazards and Safety*, M.B. Tahir, M. Sagir, and A.M. Asiri, Editors. 2021, Elsevier. p. 31-54.
4. Khan, I.; Saeed, K.Khan, I. Nanoparticles: Properties, applications and toxicities. *Arabian Journal of Chemistry*, **2019**, *12*, 908-931, https://doi.org/10.1016/j.arabjc.2017.05.011.
5. Ijaz, I.; Gilani, E.; Nazir, A.Bukhari, A. Detail review on chemical, physical and green synthesis, classification, characterizations and applications of nanoparticles. *Green Chemistry Letters and Reviews*, **2020**, *13*, 223-245, https://doi.org/10.1080/17518253.2020.1802517.
6. Lv, S.; Ma, L.; Shen, X.Tong, H. Potassium chloride-catalyzed growth of porous carbon nanotubes for high-performance supercapacitors. *Journal of Alloys and Compounds*, **2022**, *906*, 164242, https://doi.org/10.1016/j.jallcom.2022.164242.
7. Elsaid, K.; Abdelkareem, M.A.; Maghrabie, H.M.; Sayed, E.T.; Wilberforce, T.; Baroutaji, A.Olabi, A.G. Thermophysical properties of graphene-based nanofluids. *International Journal of Thermofluids*, **2021**, *10*, 100073, https://doi.org/10.1016/j.ijft.2021.100073.

8. Rahman, M.A.; Harshita; Harwansh, R.K.Deshmukh, R. Carbon-Based Nanomaterials: Carbon Nanotubes, Graphene and Fullerenes in Control of Burns Infections and Wound Healing. *Curr Pharm Biotechnol*, **2022**, https://doi.org/10.2174/1389201023666220309152340.
9. Wang, X.; Yuan, Y.; Xie, X.; Zhang, Y.; Min, C.Yuan, X. Graphene-Based Opto-Thermoelectric Tweezers. *Advanced Materials*, **2022**, *34*, 2107691, https://doi.org/10.1002/adma.202107691.
10. Liu, Y.; Zheng, Q.; Yuan, H.; Wang, S.; Yin, K.; Dai, X.; Zou, X.Jiang, L. High Sensitivity Terahertz Biosensor Based on Mode Coupling of a Graphene/Bragg Reflector Hybrid Structure. *Biosensors (Basel)*, **2021**, *11*, https://doi.org/10.3390/bios11100377.
11. Mohanta, Y.K.; Biswas, K.; Rauta, P.R.; Mishra, A.K.; De, D.; Hashem, A.; Al-Arjani, A.-B.F.; Alqarawi, A.A.; Abd-Allah, E.F.; Mahanta, S.Mohanta, T.K. Development of Graphene Oxide Nanosheets as Potential Biomaterials in Cancer Therapeutics: An In-Vitro Study Against Breast Cancer Cell Line. *Journal of Inorganic and Organometallic Polymers and Materials*, **2021**, *31*, 4236-4249, https://doi.org/10.1007/s10904-021-02046-6.
12. Mann, R.; Mitsidis, D.; Xie, Z.; Mcneilly, O.; Ng, Y.H.; Amal, R.Gunawan, C. Antibacterial Activity of Reduced Graphene Oxide. *Journal of Nanomaterials*, **2021**, *2021*, 9941577, https://doi.org/10.1155/2021/9941577.
13. Jun, Y.-S.; Habibpour, S.; Hamidinejad, M.; Park, M.G.; Ahn, W.; Yu, A.Park, C.B. Enhanced electrical and mechanical properties of graphene nano-ribbon/thermoplastic polyurethane composites. *Carbon*, **2021**, *174*, 305-316, https://doi.org/10.1016/j.carbon.2020.12.023.
14. King, J.A.; Klimek, D.R.; Miskioglu, I.Odegard, G.M. Mechanical properties of graphene nanoplatelet/epoxy composites. *Journal of Composite Materials*, **2015**, *49*, 659-668, https://doi.org/10.1177/0021998314522674.
15. Hardiansyah, A.; Yang, M.-C.; Liao, H.-L.; Cheng, Y.-W.; Destyorini, F.; Irmawati, Y.; Liu, C.-M.; Yung, M.-C.; Hsu, C.-C.Liu, T.-Y. Magnetic Graphene-Based Sheets for Bacteria Capture and Destruction Using a High-Frequency Magnetic Field. *Nanomaterials (Basel, Switzerland)*, **2020**, *10*, 674, https://doi.org/10.3390/nano10040674.
16. Evariste, L.; Braylé, P.; Mouchet, F.; Silvestre, J.; Gauthier, L.; Flahaut, E.; Pinelli, E.Barret, M. Graphene-Based Nanomaterials Modulate Internal Biofilm Interactions and Microbial Diversity. *Frontiers in Microbiology*, **2021**, *12*, https://doi.org/10.3389/fmicb.2021.623853.
17. Tu, Y.; Lv, M.; Xiu, P.; Huynh, T.; Zhang, M.; Castelli, M.; Liu, Z.; Huang, Q.; Fan, C.; Fang, H.Zhou, R. Destructive extraction of phospholipids from Escherichia coli membranes by graphene nanosheets. *Nat Nanotechnol*, **2013**, *8*, 594-601, https://doi.org/10.1038/nnano.2013.125.
18. Radhi, A.; Mohamad, D.; Abdul Rahman, F.S.; Abdullah, A.M.Hasan, H. Mechanism and factors influence of graphene-based nanomaterials antimicrobial activities and application in dentistry. *Journal of Materials Research and Technology*, **2021**, *11*, 1290-1307, https://doi.org/10.1016/j.jmrt.2021.01.093.
19. Liang, J.-Z.; Du, Q.; Tsui, G.C.-P.Tang, C.-Y. Tensile properties of graphene nanoplatelets reinforced polypropylene composites. *Composites Part B: Engineering*, **2016**, *95*, 166-171, https://doi.org/10.1016/j.compositesb.2016.04.011.
20. Mirzaei, J.; Fereidoon, A.Ghasemi-Ghalebahman, A. Experimental analysis of mechanical properties of graphene/kenaf/basalt reinforced hybrid nanocomposites using response surface methodology. *Journal of the Brazilian Society of Mechanical Sciences and Engineering*, **2021**, *43*, 215, https://doi.org/10.1007/s40430-021-02936-3.
21. Zakaria, M.R.; Abdul Kudus, M.H.; Md. Akil, H.Mohd Thirmizir, M.Z. Comparative study of graphene nanoparticle and multiwall carbon nanotube filled epoxy nanocomposites based on mechanical, thermal and dielectric properties. *Composites Part B: Engineering*, **2017**, *119*, 57-66, https://doi.org/10.1016/j.compositesb.2017.03.023.
22. Suter, J.L.Coveney, P.V. Principles governing control of aggregation and dispersion of aqueous graphene oxide. *Scientific Reports*, **2021**, *11*, 22460, https://doi.org/10.1038/s41598-021-01626-3.
23. Hernandez, C.J.; Beaupre, G.S.; Keller, T.S.Carter, D.R. The influence of bone volume fraction and ash fraction on bone strength and modulus. *Bone*, **2001**, *29*, 74-8, https://doi.org/10.1016/s8756-3282(01)00467-7.
24. Keaveny, T.M.; Morgan, E.F.; Niebur, G.L.Yeh, O.C. Biomechanics of trabecular bone. *Annu Rev Biomed Eng*, **2001**, *3*, 307-33, https://doi.org/10.1146/annurev.bioeng.3.1.307.
25. Rezwan, K.; Chen, Q.Z.; Blaker, J.J.Boccaccini, A.R. Biodegradable and bioactive porous polymer/inorganic composite scaffolds for bone tissue engineering. *Biomaterials*, **2006**, *27*, 3413-31, https://doi.org/10.1016/j.biomaterials.2006.01.039.